ARMY RESEARCH LABORATORY

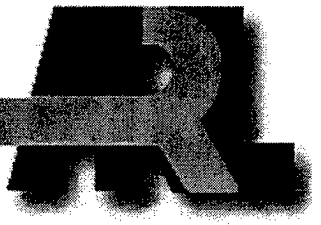

Analytical Investigation Into the Helicopter Vibration Resulting From Main Rotor Blade (MRB) Ballistic Damage

Ki C. Kim

ARL-TR-1985 JUNE 1999

19990713 147

DTIC QUALITY INSPECTED 4

Approved for public release; distribution is unlimited.

The findings in this report are not to be construed as an official Department of the Army position unless so designated by other authorized documents.

Citation of manufacturer's or trade names does not constitute an official endorsement or approval of the use thereof.

Destroy this report when it is no longer needed. Do not return it to the originator.

Army Research Laboratory
Aberdeen Proving Ground, MD 21005-5068

ARL-TR-1985 June 1999

Analytical Investigation Into the Helicopter Vibration Resulting From Main Rotor Blade (MRB) Ballistic Damage

Ki C. Kim
Survivability/Lethality Analysis Directorate

Approved for public release; distribution is unlimited.

Abstract

The effects of main rotor blade ballistic damage on helicopter vibration are investigated using a comprehensive helicopter aeroelastic analysis code. Ballistic damage to the rotor blade is represented in the blade structural model as well as in the aerodynamic analysis. Each blade is treated as being composed of elastic beams undergoing flap bending, lead-lag bending, elastic twist, and axial deflections. The dynamic response of mutli-bladed rotor systems is calculated from nonlinear periodic normal mode equations using a finite element in time scheme.

Results are calculated for a typical soft in-plane hingeless rotor helicopter with several damage configurations. Blade damage effects are determined in terms of blade mode shapes and frequencies, blade aeroelastic response, blade bending loads, and hub-fixed system vibration. Blade dissimilarity because of ballistic damage can induce a large vibratory component with its frequency the same as the rotor revolution (1/rev) on the helicopter system.

TABLE OF CONTENTS

INTENTIONALLY LEFT BLANK

LIST OF FIGURES

INTENTIONALLY LEFT BLANK

LIST OF TABLES

INTENTIONALLY LEFT BLANK

ANALYTICAL INVESTIGATION INTO THE HELICOPTER VIBRATION RESULTING FROM MAIN ROTOR BLADE (MRB) BALLISTIC DAMAGE

1. INTRODUCTION

Vibration in helicopters is a key problem facing the rotorcraft developers and users. For military helicopters in particular, vibration is of great concern since it directly affects the combat mission effectiveness of the vehicle. High vibration can cause crew discomfort and premature failures of structural components; it can increase acoustic signature, and it can reduce the aircraft's flight performance.

The principal source of vibration in the helicopter is the main rotor. In a normal operating environment, a main rotor system acts as a "filter" and transmits vibrations into the fuselage at frequencies that are integer multiples of the number of blades ($pN_b\Omega$), in which p is the integer, N_b is the number of blades, and Ω is the rotor rotational frequency. For example, for the case of the four-bladed main rotor helicopter, only 4, 8, 12, or 16 vibratory components with their frequency the same as the rotor revolution (4/rev, 8/rev, 12/rev, or 16/rev) vibrations are transmitted into the fixed system fuselage. However, when there is physical damage to the rotor blade, the rotor loses its filtering function, and all the frequencies including 1/rev, 2/rev, 3/rev, and so on, are transmitted into the helicopter fuselage, which significantly augments the vibration level. Currently, with respect to analytical vulnerability assessment, there is significant interest in the effects of ballistic damage on the performance degradation of helicopter and how damaged blades affect the helicopter vibratory loads.

The present study concentrates on an analytical investigation of the effects of individual rotor ballistic damage on helicopter system vibration. Changes in the dynamic response of the damaged blade and how these changes influence the rotor hub loads and resultant rotor-fuselage vibration are investigated in a systematic manner by using a comprehensive rotor aeroelastic analysis code. In the present study, the rotor blade and hub loads of a helicopter are calculated using the University of Maryland Advanced Rotorcraft Code (UMARC) comprehensive helicopter aeroelastic analysis code **[1]**, including blade damage effects. Then, these calculated hub loads from the UMARC analysis are used to evaluate the resulting rotor-fuselage vibrations.

Numerical results are first calculated for a typical helicopter with a baseline (undamaged) configuration. Results are then calculated for this helicopter, with representative levels of ballistic damage to one of the main rotor blades. The effects of this damage on this helicopter's

performance are determined in terms of blade modal shapes and frequencies, rotor system dynamic loads, and hub vibration levels at fixed system locations.

In the context of the U.S. Army Research Laboratory's (ARL) process structure for analyzing combat system vulnerability, this study and its associated engineering-based methods address the mapping from Level 2, the Target Component Damage State, to Level 3, the Target Capability State (i.e., O2, 3 mapping). Here, for example, physical and structural/aerodynamic factors defining rotor blade damage (Level 2) are mapped via engineering methods into parameters that define the rotor and helicopter system's functional capability (Level 3); all the defining terms are explicit and measurable through experimentation. Application of these and other engineering analysis tools to the vulnerability/lethality process structure for Level 02,3 mapping is being actively worked in the Survivability/Lethality Analysis Directorate (SLAD) of ARL.

2. NOMENCLATURE

C_w	Helicopter weight coefficient, $W / \pi R^2 \rho (\Omega R)^2$
c_0	Lift coefficient at zero angle of attack
c_1	Lift curve slope
C_d	Blade section drag coefficient
C_l	Blade section lift coefficient
$C_{m_{ac}}$	Blade section pitching moment coefficient about aerodynamic center
d_0	Viscous drag coefficient
d_1, d_2	Pressure drag coefficients
E	Young's modulus
EI_y	Flap-wise bending stiffness, *lb-in²*
EI_z	Chord-wise bending stiffness, *lb-in²*
F_x, F_y	Hub longitudinal and lateral in-plane force, respectively, *lb*
f_0, f_1	Pitching moment coefficient
G	Shear modulus
GJ	Effective sectional torsional stiffness, *lb-in²*
I_y, I_z	Blade cross-sectional moment of inertia about y and z axis, respectively, *lb*
M	Mach number
M_x, M_y	Hub rolling and pitching moment, respectively, *lb-in.*
m	Blade section mass, *slug*
m_o	Reference blade section mass, *slug*
N_b	Number of blades

p	Integer number (i.e., p = 1,2,...)
$\mathbf{q}$	Global displacement vector
R	Blade radius, *ft*
T	Rotor thrust, *lb*
u	Blade displacement in the axial direction, *ft*
v	Blade displacement in the lead-lag direction, *ft*
V	Helicopter forward speed, *ft/sec*
w	Blade displacement in the flap-wise direction, *ft*
W	Helicopter gross weight, *lb*
α	Blade section angle of attack, *radians (rad)*
α_s	Longitudinal shaft tilt relative to wind axis, *rad*
β_0	Rotor coning angle, *rad*
$\beta_{1s}\beta_{1c}$	Lateral and longitudinal rotor disk tilt angle, respectively, *rad*
$\theta_{1c}\theta_{1s}$	Lateral and longitudinal cyclic trim input, respectively, *rad*
β_l,β_d,β_m	Aerodynamic deficiency functions in lift, drag, and moment, respectively
$\theta_{.75}$	Collective blade pitch at 75% radius, *rad*
μ	Advance ratio, $V/\Omega R$
σ	Rotor solidity ratio, $N_b c_m/\pi R$
$\hat{\phi}$	Blade twist, *rad/ft*
ϕ_s	Lateral shaft tilt, *rad*
Ψ	Rotor azimuthal angle, *degree*
ρ	Air density, $slug/ft^3$
Ω	Rotor rotational speed, *rad/sec*
θ_{tr}	Tail rotor collective control setting, *rad*

3. ANALYSIS

In this section, the underlying physics of the damaged rotor blade dynamics and their effects on fixed system rotor motion are briefly summarized, followed by the formulation of the problem for assessing the effects of blade damage on the helicopter vibration.

Understanding the individual blade's motion is of central importance to gain insights into the rotor imbalance problem: how the certain type of rotor blade damage affects the blade and rotor motions. In addition, this fundamental understanding can provide the preliminary intuitions to the problem and help to establish the guideline for the results obtained from more complicated analyses.

3.1 Background

When a helicopter main rotor blade is sufficiently damaged (e.g., in combat, by a ballistic high-explosive projectile), rotor system dynamic imbalance (inertial and/or aerodynamic) occurs. This results in undesirable asymmetrical forces and motions that affect the vibration of helicopters.

If all the blades are undamaged, ideally, the blade responses will be identical. For example, for a four-bladed rotor, the summation of the individual blade response will be zero for harmonics 1, 2, and 3. This is the well-known cancellation effect existing in a periodic system.**[2]** However, if there is damage to the rotor and all the blade responses are not equal, then no cancellation occurs. Therefore, the 1, 2, and 3/rev frequency vibration effects are felt in the fixed system. These additional frequencies transmitted will cause the helicopter to shake and create mechanical vibrations. In addition, there will be physiological effects on humans subjected to these vibrations; natural frequencies of the helicopter will change with possible aeroelastic instabilities, structural fatigue life may be reduced by increased vibrations, and general helicopter performance will be degraded.

3.2 Rigid Flapping Blade Model

The mathematical model used for the rigid blade model is illustrated in Figure 1. The helicopter rotor blade is modeled as a rigid blade rotating at a constant angular velocity Ω. Each blade is represented as a flapping mass on a blade length with a root effective flap hinge and a root angular spring.**[3]** In addition, the rotor system hub mass is represented to include fuselage motion effects. The purpose of this simple model is to illustrate the basic phenomenon of frequency transformation from a rotating (blade) system to a nonrotating (hub) system.

For an undamaged rotor system, we can assume that the root reaction of nth blade (n=1 to N_b) is a periodic function of $\Psi_n = \Psi + n\Delta\Psi$ $\left(\Delta\Psi = 2\pi / N_b\right)$. Therefore, all the blades have identical loading and motion. Using a Fourier series analysis for a periodic system, one can find a certain basic fundamental pattern involving the coordinate transformation rule between a rotating frame and a nonrotating frame. This is summarized in Table 1. As shown in Table 1, the pN_b/rev hub drag and side forces (p is an integer) in a fixed system (nonrotating) are coming from $pN_b \pm 1$/rev rotating blade in-plane shear forces. Likewise, pN_b/rev hub pitch and roll moments in a fixed system are attributable to $pN_b \pm 1$/rev rotating blade flapping moments. For the rotor thrust and torque transmitted through the hub, there is no ± 1/rev conversion as shown in the

table. This is because these quantities are independent of the coordinate transformation between the rotating frame and the nonrotating (fixed) frame.

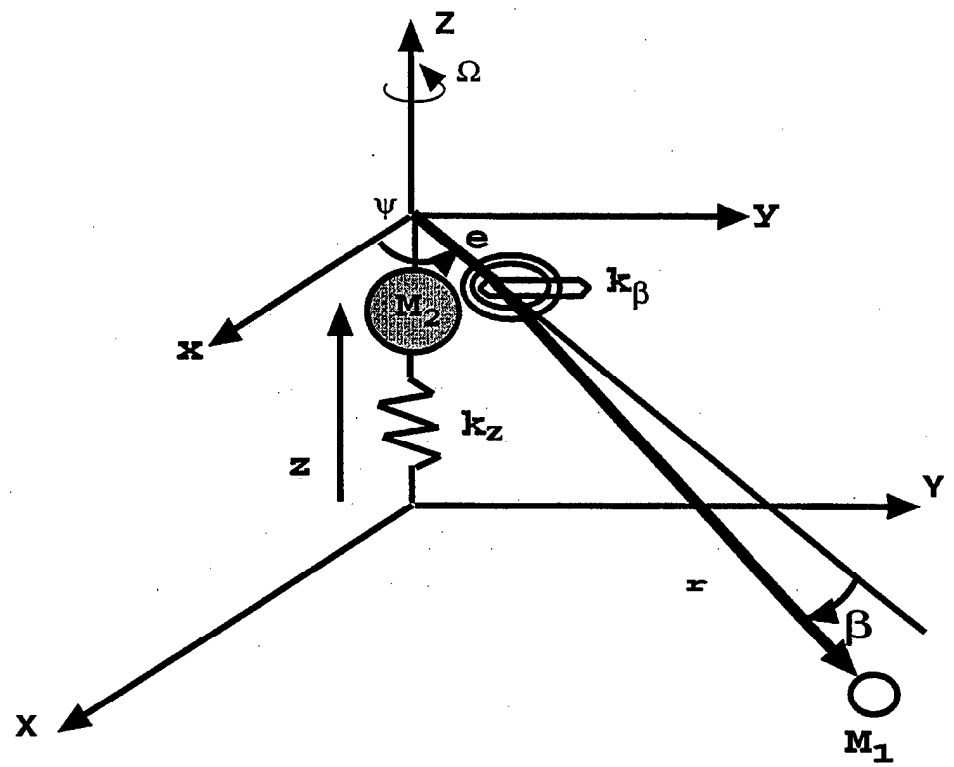

Figure 1. Rigid Flapping Rotor Blade Model With Hinge Offset and Spring.

Table 1. Vibration Transmission Through Rotor Hub

Fixed System (non-rotating)		Rotating System
Thrust at pN_b/rev	Attributable to	Vertical Shear at pN_b/rev
Rotor Drag and Side Forces at pN_b/rev	Attributable to	In-plane Shears at $pN_b \pm 1$/rev
Torque at pN_b/rev	Attributable to	Lag Moment at pN_b/rev
Hub Pitch and Roll Moments at pN_b/rev	Attributable to	Flap-wise Moment at $pN_b \pm 1$/rev

For a damaged rotor system where the dissimilarities between blades are present, one must consider the motions of all blades. Let us qualitatively examine the hub moments of a four-bladed rotor system with and without blade damage. Tables 2 and 3 show the harmonic contents of hub moments for an undamaged and damaged rotor system. Comparing the two tables, we see an

interesting phenomenon: Table 3 is filled with more terms than Table 2. This indicates that more frequencies are transmitted into the fixed system when the blades are damaged than when they are undamaged. Therefore, when a blade is damaged, the helicopter is subject to these additional frequencies forcing through the hub.

With the damaged blade, the 4/rev hub moments attributable to 3 and 5/rev flapwise moments are still present. However, the effect to be noted is that all the frequencies are coming through to the fixed system when a blade is damaged (i.e., 1, 2, 3, 4, 5, 6/rev), as shown in Table 3. In other words, one must address other frequency components besides the pN_b/rev frequency forcing for the helicopter vibration study involving rotor blade damage.

Table 2. Fixed System Hub Moments Attributable to Blade Flapping Moments (undamaged)

Hub Moments	Rotating Flapping Frequency				
	1/rev	2/rev	3/rev	4/rev	5/rev
1/rev					
2/rev					
3/rev					
4/rev			⊗		⊗
5/rev					
6/rev					

Table 3. Fixed System Hub Moments Attributable to Blade Flapping Moments (damaged)

Hub Moments	Rotating Flapping Frequency				
	1/rev	2/rev	3/rev	4/rev	5/rev
1/rev		⊗			
2/rev	⊗		⊗		
3/rev		⊗		⊗	
4/rev			⊗		⊗
5/rev				⊗	
6/rev					⊗

In the next section, more refined blade model for the rotor system is presented to examine the realistic motion of the blade and to analyze the blade aeroelastic response and associated blade/hub loads.

3.3 Coupled Flap-Lag-Torsion Elastic Blade Model

Calculation of aeroelastic response of the blade is an essential intermediate step to calculate the blade and hub loads and ultimately, helicopter vibration. In the present study, the UMARC, a comprehensive helicopter aeroelastic analysis code based on finite element theory in space and time **[1]**, is used. In UMARC, the blade is modeled as an elastic beam undergoing flap bending, lag bending, elastic twist, and axial deflections. The fuselage is assumed to be a rigid body undergoing six degrees of freedom movement. Each blade is discretized into a number of beam elements, and for each element there is a continuity of displacement and slope for flap (w) and lag (v) deflections and a continuity of displacement for axial (u) and torsional ($\hat{\phi}$) deflections. There are two internal nodes for axial displacement and one for elastic twist, resulting in a total of 15 degrees of freedom for each element.

3.3.1 *Formulation*

The formulation for the blade and fuselage equations of motion is based on Hamilton's principle:

$$\int_{t_1}^{t_2} (\delta U - \delta T - \delta W)\, dt = 0 \tag{1}$$

in which δU, δT, and δW are, respectively, the variations in the strain energy, the kinetic energy, and the virtual work done by external forces. The expressions for δU and δT are given in Reference 1. The virtual work δW can be expressed as

$$\delta W = \int_0^R \left(L_u^A \delta u + L_v^A \delta v + L_w^A \delta w + M_\phi^A \delta \phi \right) dx \tag{2}$$

in which L_u^A, L_v^A, L_w^A, and M_ϕ^A are the external aerodynamic loads distributed along the length of the blade in the axial, lead-lag, flap, and torsional directions, respectively.

Aerodynamic loads are calculated using quasi-steady strip theory. Noncirculatory aerodynamic forces are also included. For the calculation of the rotor inflow, a linear wake model is used. Aerodynamic coefficients are computed in the form of analytical expressions as well as data tables. These are represented as

$$
\begin{aligned}
C_l &= c_0(\alpha, M, \mathbf{q}, \dot{\mathbf{q}}) + c_1(\alpha, M, \mathbf{q}, \dot{\mathbf{q}})\alpha \\
C_d &= d_0(\alpha, M, \mathbf{q}, \dot{\mathbf{q}}) + d_1(\alpha, M, \mathbf{q}, \dot{\mathbf{q}})\alpha + d_2(\alpha, M, \mathbf{q}, \dot{\mathbf{q}})\alpha^2 \\
C_{m_{ac}} &= f_0(\alpha, M, \mathbf{q}, \dot{\mathbf{q}}) + f_1(\alpha, M, \mathbf{q}, \dot{\mathbf{q}})\alpha
\end{aligned}
\tag{3}
$$

in which $\mathbf{q}$ and $\dot{\mathbf{q}}$ are arrays of nodal displacements and velocity vectors, respectively. Equation (3) represents a set of nonlinear aerodynamic coefficients, including effects of blade motion and Mach number.

For the calculation of aerodynamic forces on the damaged blade, recently completed wind tunnel test data were used in the form of data table look-up (Eq. 3). The details of the test and data acquisition reduction are available in References 4 and 5.

3.3.2 *Aeroelastic Analysis*

The rotor response analysis consists of two phases, vehicle trim and steady response, and is calculated as one coupled solution using a modified Newton method.

3.3.3 *Vehicle Trim*

Propulsive trim, which simulates the free flight condition of the vehicle, is used to calculate rotor control settings. The solution is determined from vehicle overall equilibrium equations: three force (vertical, longitudinal, and lateral), and three moment (pitch, roll and yaw) equations. For a specified weight coefficient (C_w) and advance ratio (μ), the trim solution calculates the shaft tilt angles (α_s, ϕ_s), the pitch control settings (θ_0, θ_{1c}, θ_{1s},), and the tail rotor thrust (θ_{tr}).

These trim values are calculated iteratively using the modified hub forces and moments including the blade elastic responses.

3.3.4 *Steady Periodic Response*

The steady response involves the determination of time-dependent blade positions at different azimuth locations for one rotor revolution. To reduce computational time, the finite element equations are transformed into normal mode equations, based on the coupled natural vibration characteristics of the blade. These nonlinear periodic coupled equations are solved for steady response using a finite element in time procedure based on Hamilton's principle in weak form. One rotor revolution is divided into a number of azimuthal elements, and then periodicity of response is used to join the motions of the first and last elements. The assembly of elements

results in nonlinear algebraic equations that are solved using the Newton-Raphson procedure (for details, see Ref. 6).

3.4 Modeling and Analysis of a Damaged Rotor System

Most of the comprehensive aeroelastic codes developed to calculate helicopter dynamic response and stability employ the assumption that the response of all the blades is identical with an appropriate phase shift for each blade. Thus, in the rotor response calculation, a set of coupled flap-lag-torsion equations corresponding to a single blade is used. In the study of a ballistically damaged rotor system, the motion of each blade has to be represented by an independent set of equations, and their response has to be calculated individually. Otherwise, an individual blade cannot be represented. This type of solution approach is referred as a "multi-blade formulation." This formulation also drastically increases the size of equations to be solved. For example, the size of the system equations quadruples for a four-bladed rotor. In the present study, a multi-blade formulation developed in Reference 3 is used to calculate the rotor hub forces and moments. Therefore, the motions of the individual blades are considered in the calculation of hub loads and moments.

3.4.1 *Rotor Blade Ballistic Damage Model*

Ballistic damage to a rotor blade can range from a simple hole type damage to more complex shape damage involving skin delaminations, irregular material removal, rugged edge shapes, etc. In the present study, damage to the blade is represented as a reduction in structural properties as well as a change in aerodynamic characteristics of blade. The structural damage is simulated by reducing the mass, bending, and torsional stiffnesses (m_0, EI_y, EI_z, and GJ) of a damaged blade section. These values are estimated, based on the prescribed damaged configuration, either observed from ballistic tests or by an analytical method, and are used as input to the UMARC code.

The aerodynamic damage is simulated as a change in blade aerodynamic lift, drag, and moment characteristics. A method used in Reference 7 is adopted to represent ballistic damage effects on blade aerodynamics. The following relations are used to modify the change in aerodynamic coefficients of the damaged blade:

$$\begin{aligned} C_{l\text{damaged}} &= \beta_l C_{l\text{undamaged}} \\ C_{d\text{damaged}} &= \beta_d C_{d\text{undamaged}} \\ C_{m_{ac}\text{damaged}} &= \beta_m C_{m_{ac}\text{undamaged}} \end{aligned} \tag{4}$$

in which β_t, β_d, β_m are, respectively, the lift, drag, and moment deficiency functions. These are estimated, based on the wind tunnel test results.**[4-5]**

The ballistic damage model used in this study is constructed in a global manner. It is based on the assumption that ballistic damage to a rotor blade can be collectively represented as stiffness reductions as well as material discontinuities. More elaborate treatments of individual failure mode, including assessing blade structural integrity, requires additional structural modeling such as **NA**tional Aeronautics and Space Administration **STR**uctural **AN**alysis (NASTRAN) or ALGOR (not an acronym).**[8-9]** The major objectives of the present modeling approach are to represent the level of degradation in the rotor blade beam model attributable to ballistic damage and to investigate the effects on overall rotor and helicopter's performance (i.e., 02,3 mapping).

4. RESULTS AND DISCUSSION

Numerical results are obtained for a four-bladed soft in-plane hingeless main rotor helicopter. Results are first calculated for an undamaged (baseline) rotor configuration. Results then are calculated for this rotor with simulated blade damage conditions, and the effects of damages are assessed. Some important parameters of the helicopter rotor used in the present study are given in Table 4.

Table 4. Hingeless Rotor Data

Number of blades, N	4
Rotor diameter, d	32 ft 4 in
Chord/radius, c/R	0.055
Solidity, σ	0.07
Lock number, γ	5.2
Thrust ratio, C_T/σ	0.07
Tip speed, $\Omega_{ref}R$	650 ft/sec
Blade flap inertia, I_β	162 slug-ft^2
Blade reference mass, m_0	0.115 slug/ft
Blade lift coefficient, C_l	5.73 α
Blade drag coefficient, C_d	0.0095 + 0.2 α^2
Blade pitching moment, C_m	0.0
Flap-wise stiffness, $EI_y/m\Omega^2R^4$	0.0108
Lag-wise stiffness, $EI_z/m\Omega^2R^4$	0.0268
Torsional stiffness, $GJ/m\Omega^2R^4$	0.0062

For the calculation of a dynamic response, each rotor blade is discretized into five beam elements, resulting in a total of 20 beam elements for a four-bladed rotor system. For normal mode reduction, six coupled rotating natural modes are used, primarily comprised of three flaps, two lags, and one torsion mode. For periodic response, one cycle of time is discretized into eight time elements, and each time element represents a fifth order polynomial distribution of motion.

4.1 Blade Damage Cases

The following types of ballistic damage are examined in the present study.

4.1.1 *Blade With Its Tip Loss*

Damage is assumed to be imposed on one of the four blades by removing the outboard portion of the blade, thus resulting in blade mass and length loss. For instance, 20% damage represents a blade with a loss of 20% of the blade mass and the loss of 20% of the blade radius. Damage cases involving blade tip loss considered are

CaseS1: Loss of 5% blade tip
CaseS2: Loss of 10% blade tip
CaseS3: Loss of 15% blade tip
CaseS4: Loss of 20% blade tip

4.1.2 *Blade With Hole(s) With Skin Delaminations*

This type of damage is simulated as reductions in structural load-bearing capabilities of the blade. The bending and torsional stiffness (EI_y, EI_z, and GJ) and blade mass of the 3-foot section of the blade, 20% of the blade length, are reduced by half. In addition, the location of the damage is varied from root to tip of the blade to investigate the aeroelastic characteristics of damaged blades (see Figure 2). Damage cases involving a blade with holes, as considered in the present study, are

CaseD1: Damage occurring in the root section of the blade
CaseD2: Damage occurring in the mid-span of the blade
CaseD3: Damage occurring in the outer 20% of the blade
CaseD4: This case is the same as CaseD3 but without stiffness reduction. This case is considered only to evaluate the mass loss effects alone on blade dynamics.

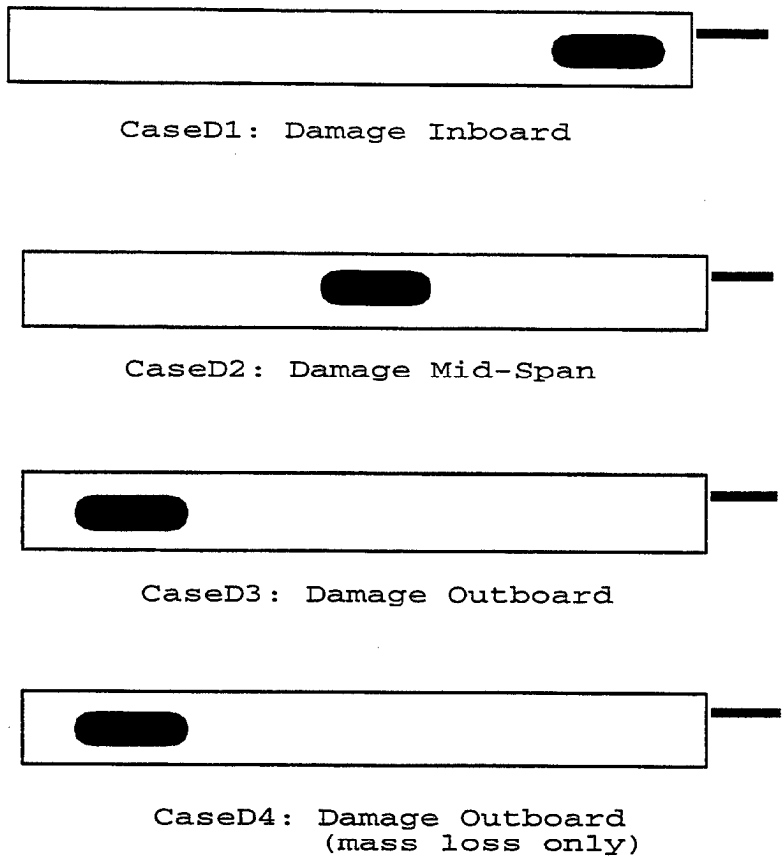

Figure 2. Schematic of Blade Damage Cases.

4.2 The Effects of Damage on Blade Vibration Characteristics

4.2.1 *Blade Tip Severance (CaseS1, CaseS2, CaseS3, CaseS4)*

The effects of blade tip loss on the blade rotating natural frequencies are summarized in Table 5. For comparison purposes, the results of the baseline (undamaged) blade are also shown, along with the four blade tip loss damage conditions: 5% (CaseS1), 10% (CaseS2), 15% (CaseS3), and 20% damage (CaseS4). It is shown that blade tip loss increases the natural frequencies of the blade. This is most likely because of the shortening of the blade. As the damage size (percent) increases, the frequencies of these modes also increase. It is also shown that the effects on blade damage are more distinct for the higher modes. Figure 3 shows the variations of the flap modes as a function of the amount of tip loss. As seen in this figure, the effects of blade loss on higher flap modes are quite significant. Figure 4 shows the variations of the in-plane mode (lag) frequencies attributable to blade tip loss. The effect of tip loss on the rigid lag mode is small, compared to a higher mode (second lag mode). Of particular interest is the behavior of the

torsional frequency of the blade, since the torsional motion is very important in blade aeroelastic stability. As the amount of tip loss increases, the frequency of the torsional mode increases, as shown in Figure 5. Again, this is thought to be most likely caused by shortening of a blade.

Table 5. The Effects of Tip Loss on Blade Natural Frequencies (per revolution)

Mode	Baseline	CaseS1	CaseS2	CaseS3	CaseS4
First Lag Mode (rigid)	0.744	0.802	0.87	0.954	1.055
First Flap Mode (rigid)	1.146	1.164	1.186	1.215	1.250
Second Flap Mode	3.512	3.698	3.928	4.213	4.571
Second Lag Mode	4.447	4.804	5.235	5.758	6.398
First Torsion Mode	4.551	4.789	5.055	5.353	5.690
Third Flap Mode	7.944	8.587	9.360	10.298	11.457

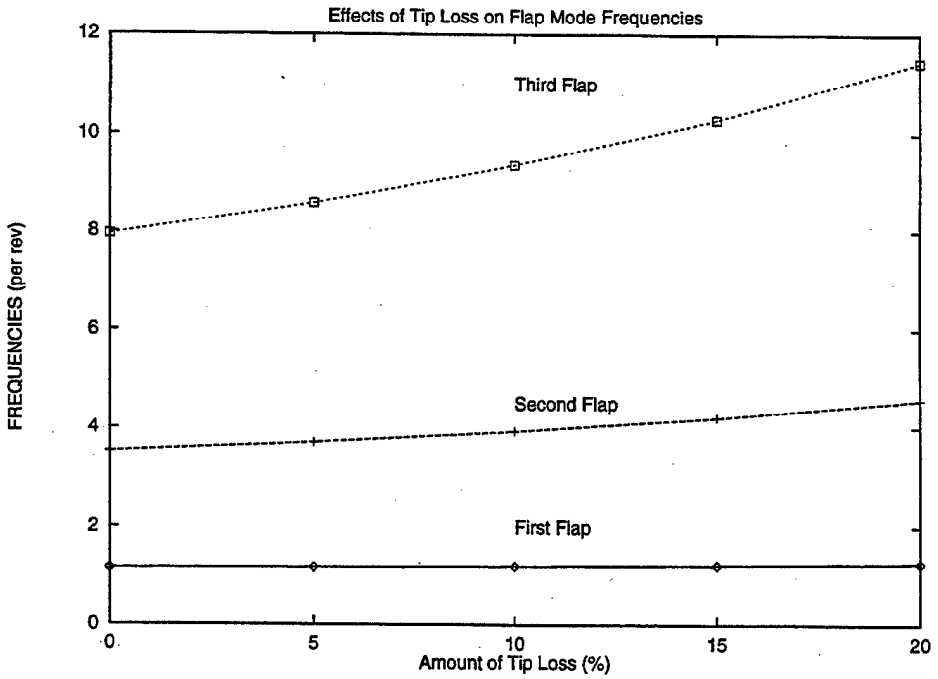

Figure 3. The Effects of Tip Loss on Flap Mode Frequencies.

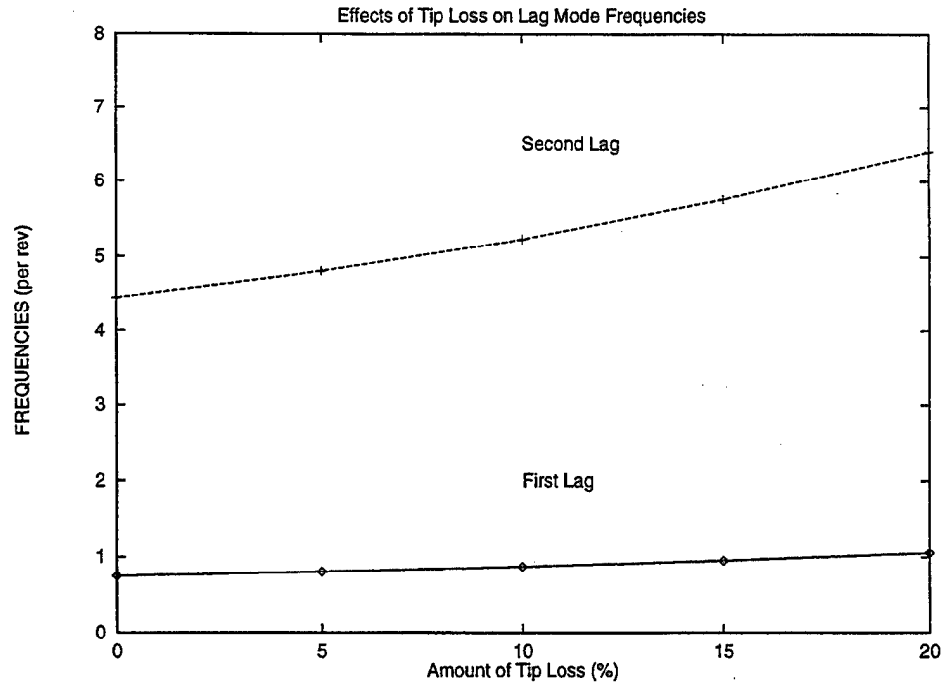

Figure 4. The Effects of Tip Loss on Lag Mode Frequencies.

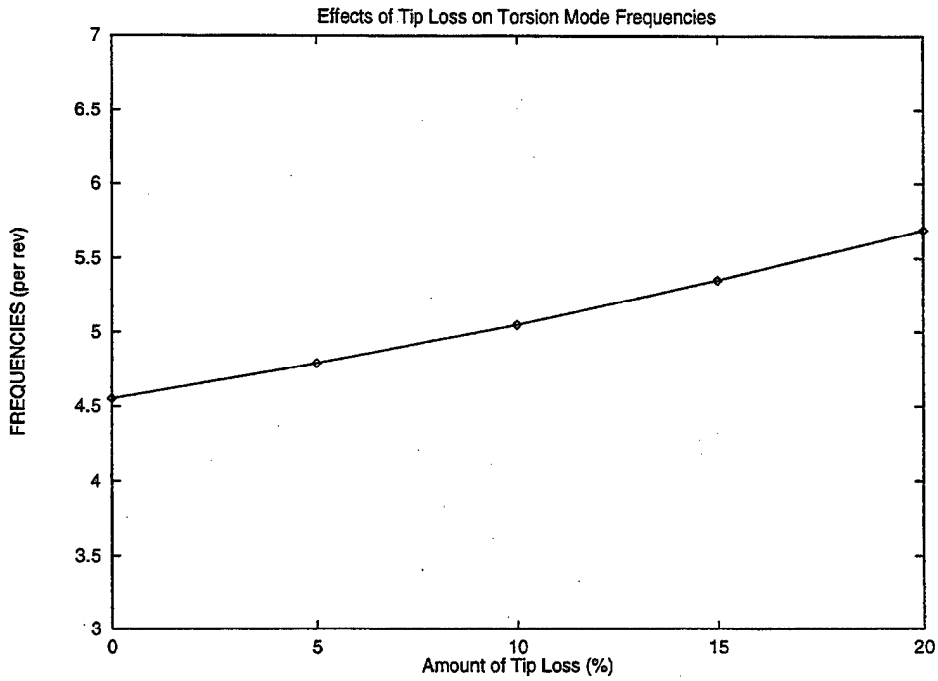

Figure 5. The Effects of Tip Loss on Torsional Mode Frequency.

4.2.2 *Blades With Hole-Type Damage (CaseD1, CaseD2, CaseD3, CaseD4)*

The effects of the blade damage on the blade rotating natural frequencies are summarized in Table 6. Again, for comparison purposes, the results of the baseline (undamaged) blade are also shown along with the four damage cases: CaseD1, CaseD2, CaseD3, and CaseD4. Some interesting phenomena are observed from the results. First, the effects of hole-type damage on blade natural frequencies are smaller as compared to the results of blade tip loss cases (see Table 5). Second, when a blade is damaged in the in-board section, the natural frequencies of the blade decrease. This is most likely because of structural softening of the blade. It is also shown that the natural frequencies increase as the location of the damage is varied from in board to out board toward the tip. Comparing the results of CaseD3 and CaseD4, it is found that when the damage occurs in the outboard section of a blade, the dominating factor affecting the natural frequencies is the inertial (mass) effect. This is attributable to the fact that the centrifugal force dominates at the tip region. Figure 6 shows the first flap mode shapes of the undamaged blade and three damage cases. Results of the second and the third flap mode shapes are shown in Figures 7 and 8, respectively. It is also shown that the effects on blade damage are more distinct for the higher modes, as shown in Figure 8. The variations of the in-plane mode shapes are shown in Figures 9 and 10, and the torsional mode shapes of the undamaged and damaged blades are shown in Figure 11.

Table 6. The Effects of Hole-Type Damage on Blade Natural Frequencies (per revolution)

Mode	Baseline	CaseD1	CaseD2	CaseD3	CaseD4
First Lag Mode (rigid)	0.744	0.612	0.747	0.848	0.848
First Flap Mode (rigid)	1.1.46	1.105	1.148	1.179	1.179
Second Flap Mode	3.512	3.387	3.674	3.562	3.581
Second Lag Mode	4.447	4.199	4.543	4.69	4.718
First Torsion Mode	4.551	3.939	4.44	5.348	5.049
Third Flap Mode	7.944	7.757	7.883	7.898	8.137

4.3 Blade Aeroelastic Responses and Loads

Calculation of blade aeroelastic response and loads requires the modeling of the aerodynamic force on the rotor blade. The details of aerodynamic analysis of a damaged blade are reported in the previous chapter (see Section 3.4). Table 7 shows values used in the present study to represent the changes in blade sectional aerodynamics attributable to damage.

Blade aeroelastic responses and loads are shown for the hole-type damage cases in which the damage effects on blade aerodynamic and structural load variations are significant. Results for blade tip loss cases are available in Reference 10.

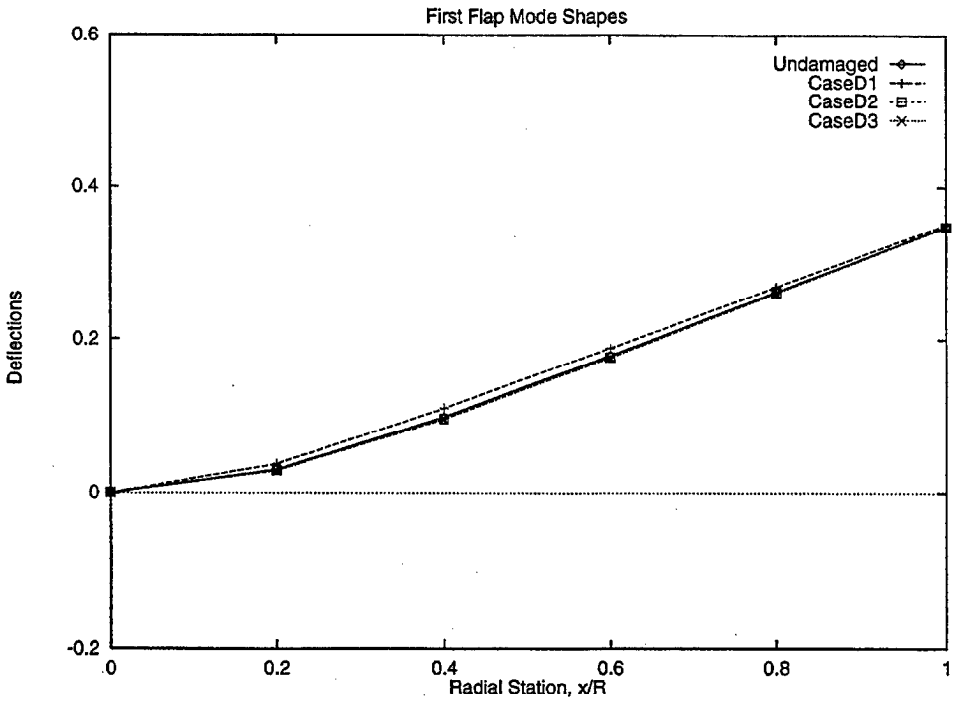

Figure 6. First Flap Mode Shapes of Undamaged and Damaged Blades.

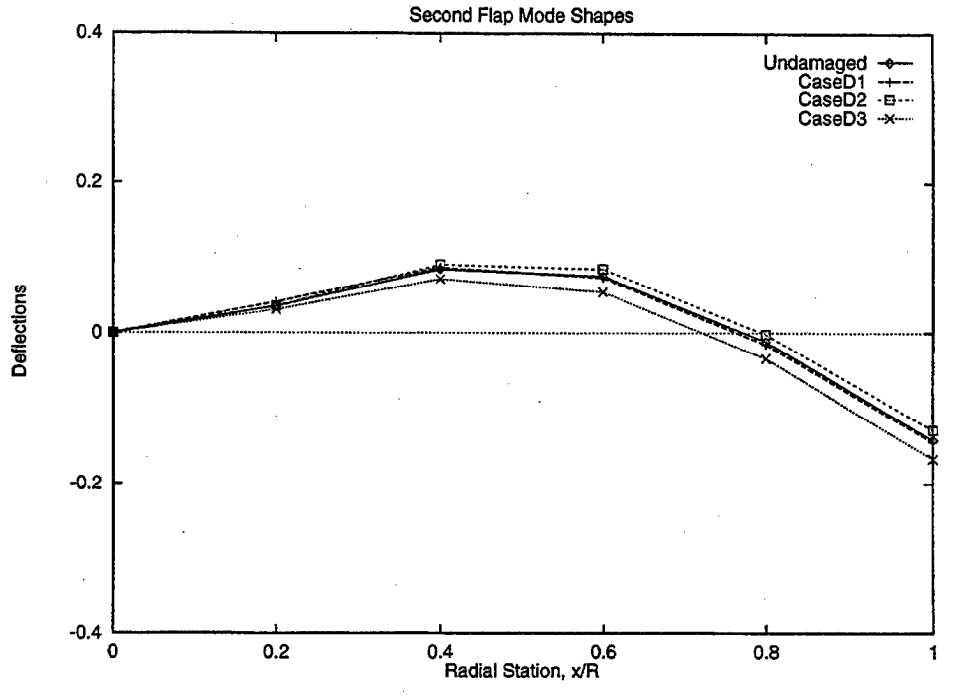

Figure 7. Second Flap Mode Shapes of Undamaged and Damaged Blades.

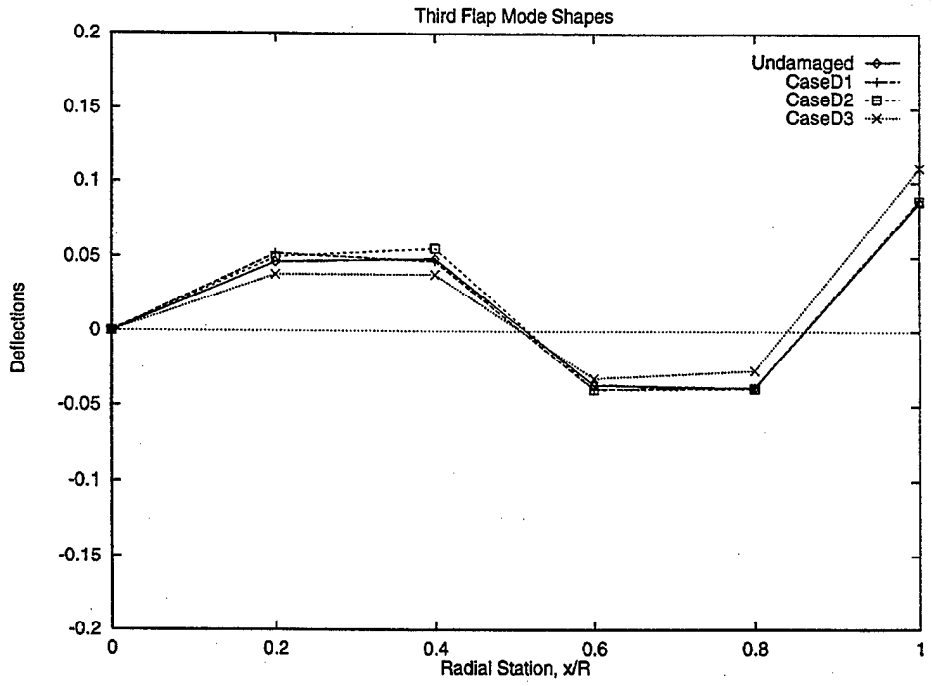

Figure 8. Third Flap Mode Shapes of Undamaged and Damaged Blades.

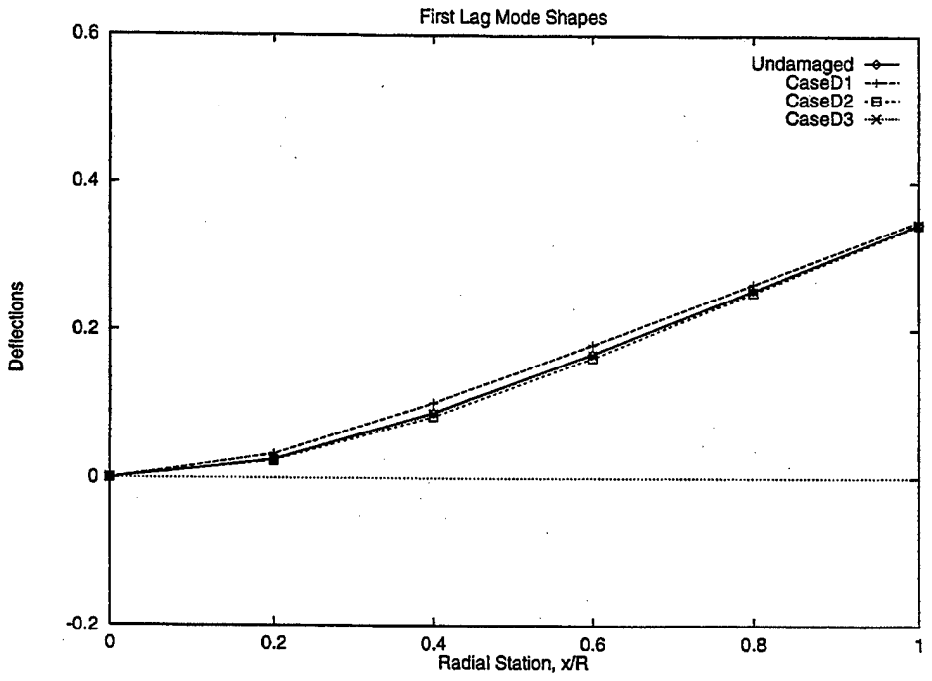

Figure 9. First Lag Mode Shapes of Undamaged and Damaged Blades.

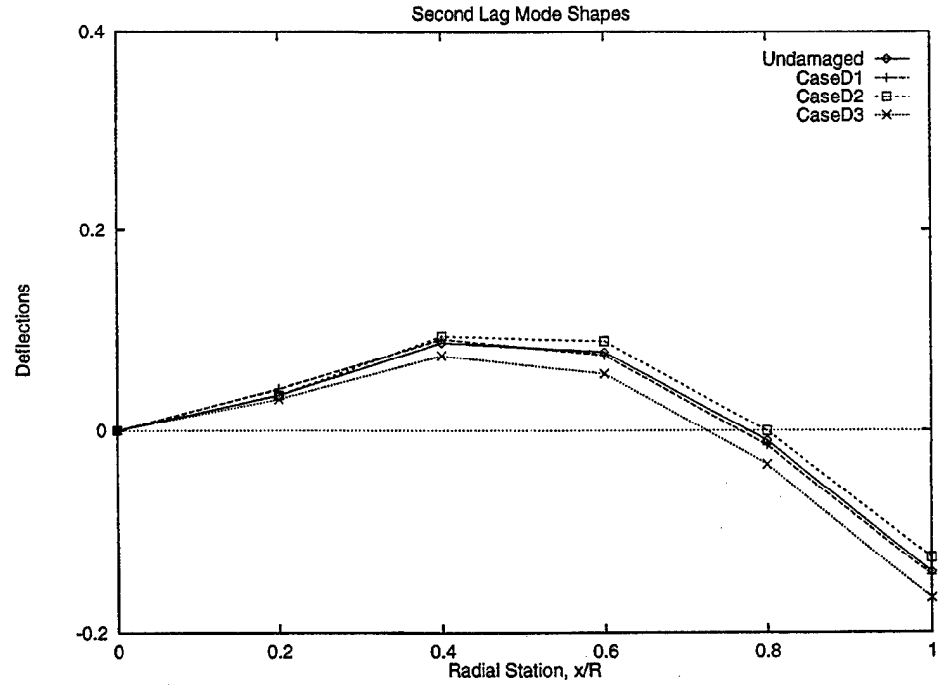

Figure 10. Second Lag Mode Shapes of Undamaged and Damaged Blades.

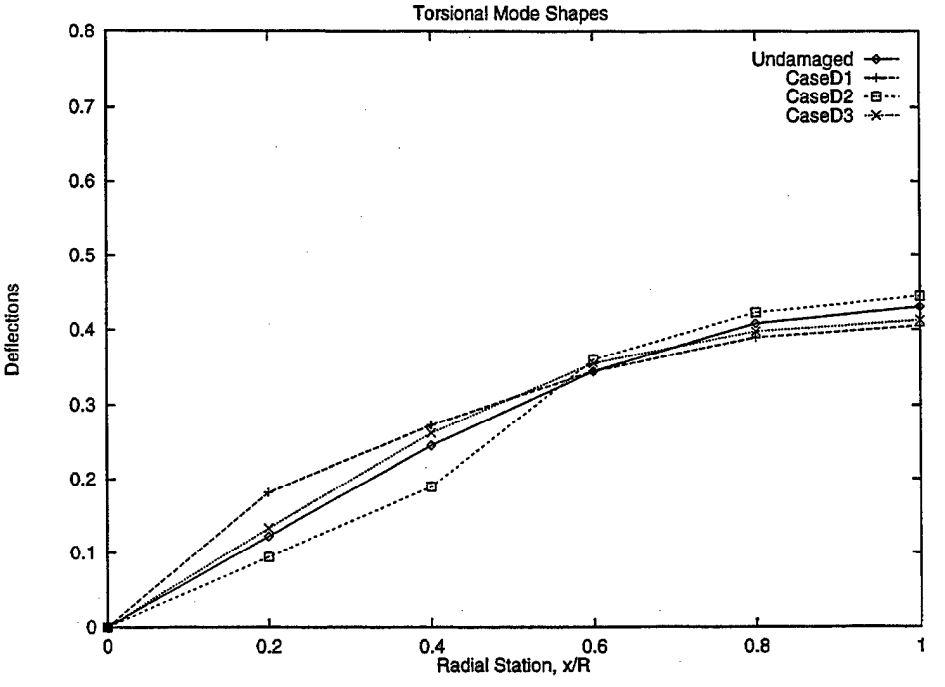

Figure 11. Torsional Mode Shapes of Undamaged and Damaged Blades.

Table 7. Aerodynamic Deficiency Functions of Damaged Airfoil

Deficiency Functions	$M_{inc} \leq 0.7$	$M_{inc} > 0.7$
β_l	0.78	$\frac{0.78}{\sqrt{1-M^2}}$
β_d	2.5	$\frac{2.5}{\sqrt{1-M^2}}$
β_m	0.92	$\frac{0.92}{\sqrt{1-M^2}}$

The flap, lag, and torsional deflections at the tip are shown in Figures 12 through 14 for the hovering flight condition ($\mu = 0.0$). Results of three different damage cases (CaseD1, CaseD2, CaseD3) are plotted along with the baseline (undamaged) values. These deflections are blade structural responses to aerodynamic loading (i.e., aeroelastic response). The amplitudes of flap-wise, lag-wise, and torsional deflections are shown to be constant for hover. Because of blade damage, there are noticeable differences in the flap amplitudes. It is seen that flapping amplitudes increase as the location of the damage moves out board. This is most likely because of high dynamic pressure at the tip region. Damage also changes the amplitudes of lag and torsional responses as shown in Figures 13 and 14.

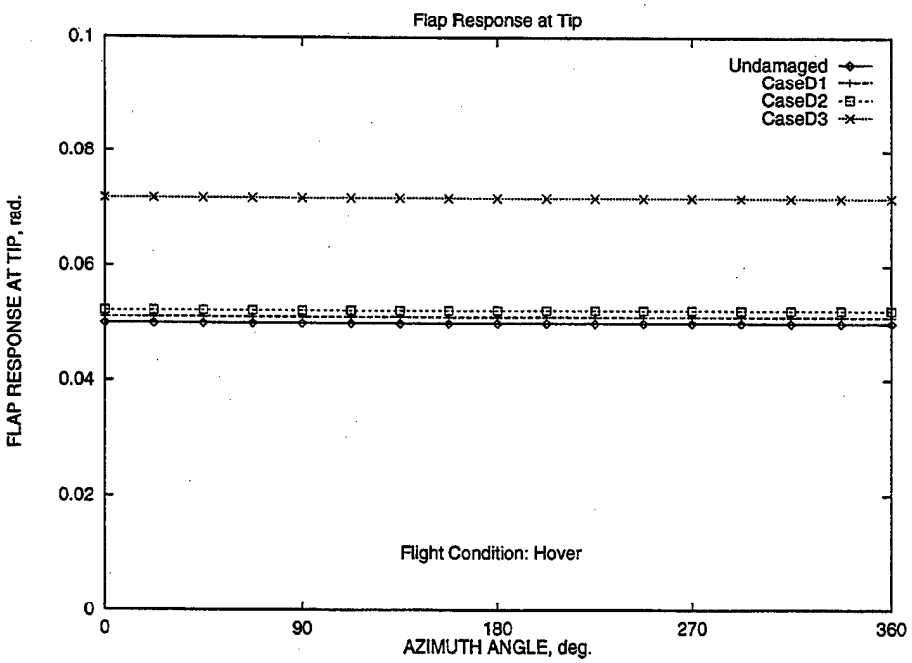

Figure 12. Flap Responses at the Tip of Undamaged and Damaged Blades in Hover ($\mu = 0$).

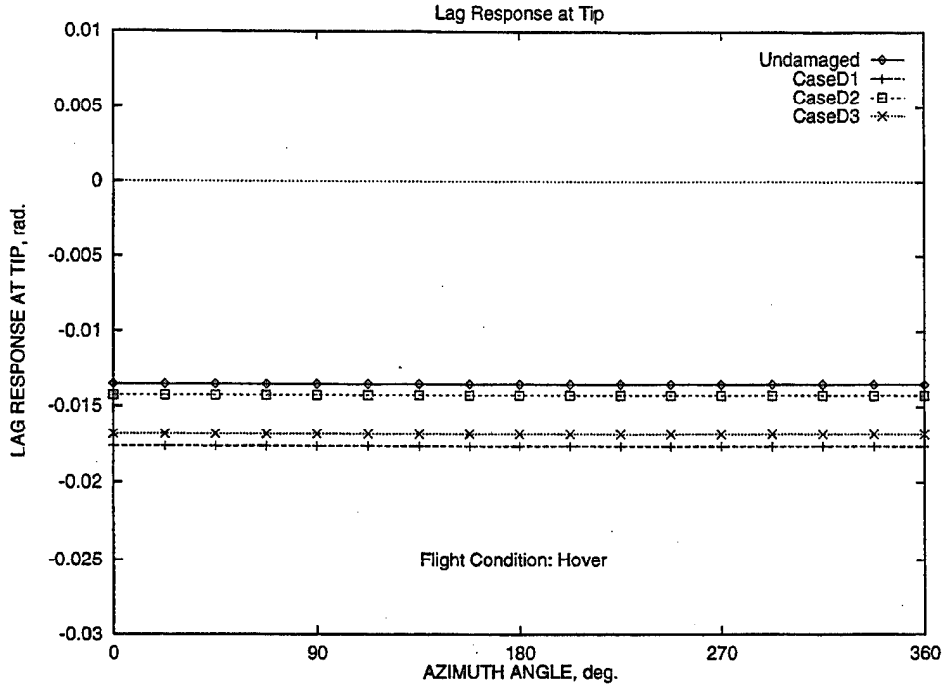

Figure 13. Lag Responses at the Tip of Undamaged and Damaged Blades in Hover ($\mu = 0$).

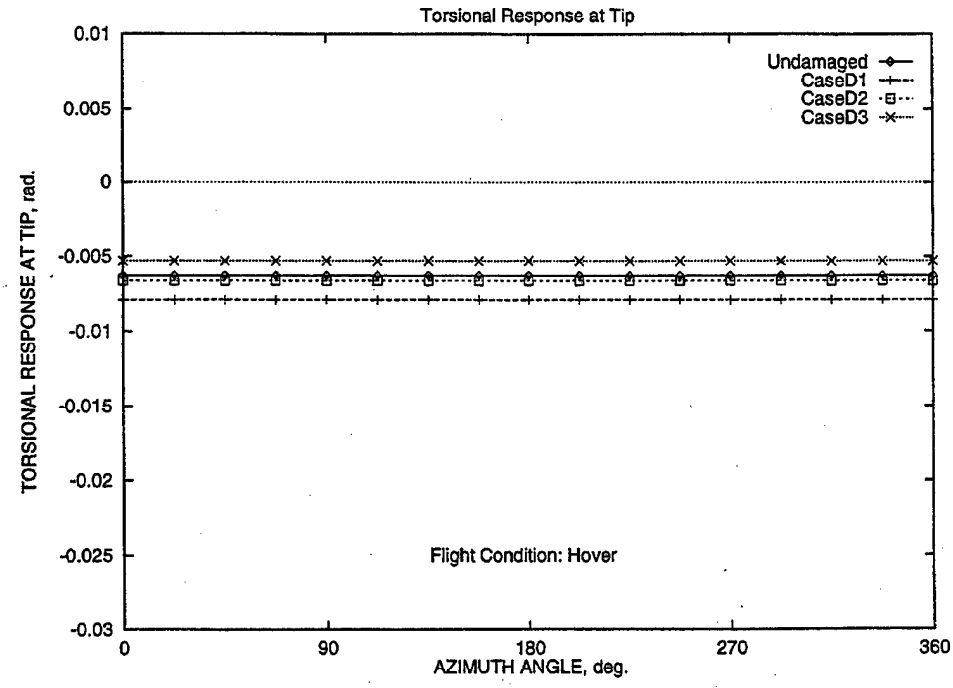

Figure 14. Torsional Responses at the Tip of Undamaged and Damaged Blades in Hover ($\mu = 0$).

Flap deflections at blade tip for forward flight conditions are shown in Figure 15 for low speed flight ($\mu = 0.1$) and Figure 16 for high speed flight ($\mu = 0.3$), respectively. Flap responses of the blade with outboard tip damage (CaseD3) are shown, along with those of the baseline case. It is seen that the effects of blade damage on flap response increase as the vehicle's speed increases. This is quite interesting and is most likely attributable to large variations of blade aerodynamic loads in a high speed flight regime.

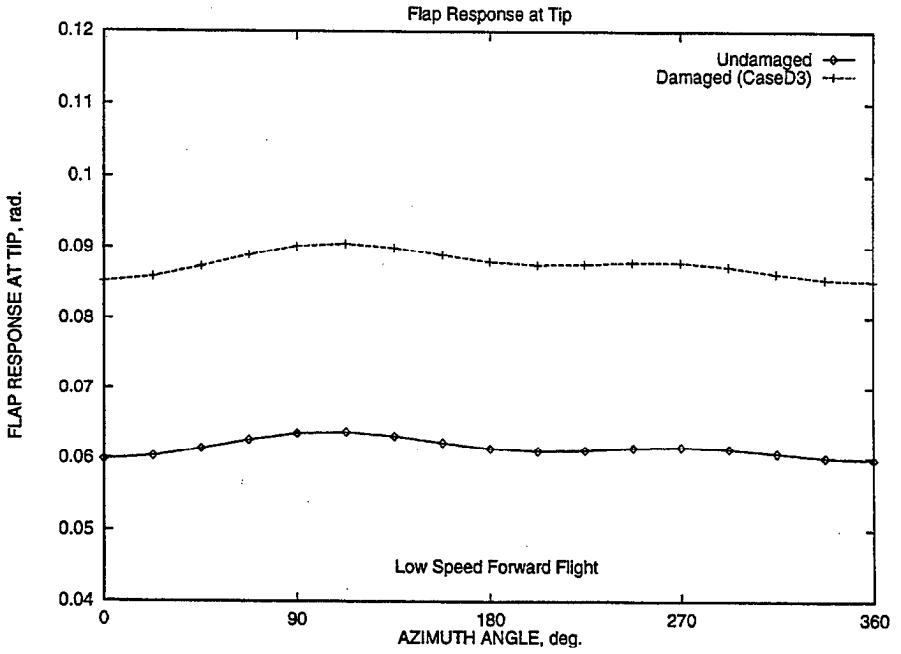

Figure 15. Flap Deflections of Undamaged and Damaged Blades in Forward Flight ($\mu = 0.1$).

The time history of blade bending moment (nondimensionalized by $m\Omega^2R^3$) variations for both undamaged and damaged case (CaseD3) are shown in Figures 17 through 20. Flap bending moments acting on the blade root are shown for two flight speed conditions in Figure 17 ($\mu = 0.1$) and Figure 18 ($\mu = 0.3$). Results of the in-plane bending moments are shown in Figures 19 and 20. These moments were calculated by radially integrating the inertial, structural, and aerodynamic forces acting along the blade (force summation method). These moments were also calculated about the deflected position of the blade. Therefore, they contained all the aeroelastic response information of the rotor system, including rotor controls and wake distributions. It is shown that the effects of blade damage on blade bendings are quite large. For example, the peak-to-peak amplitude of flap bending moment is increased by about 200% for the damaged blade as shown in Figure 18. One also observes that the peak-to-peak amplitudes of these moments are increased as the vehicle's forward speed increases.

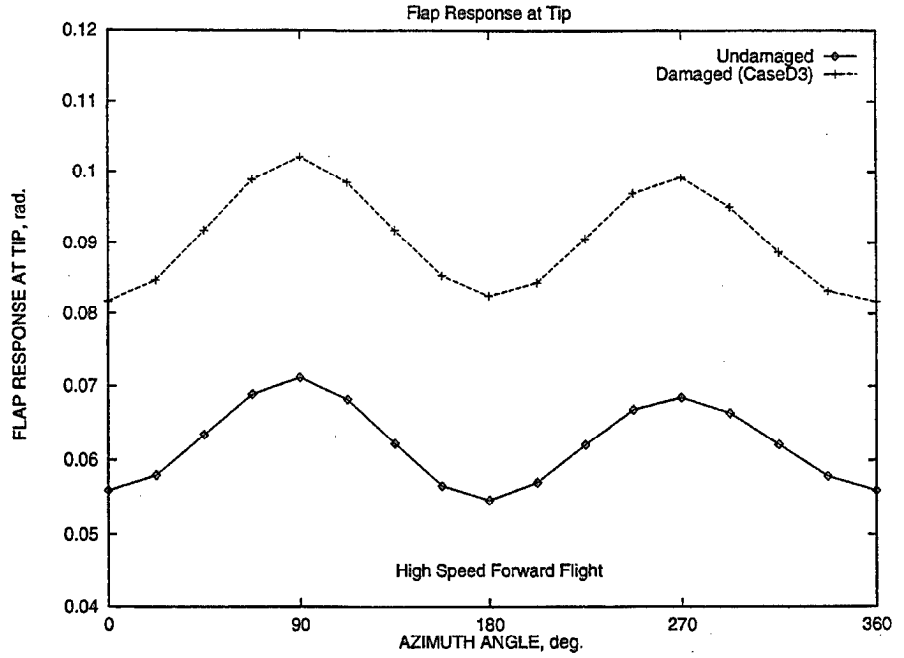

Figure 16. Flap Deflections of Undamaged and Damaged Blades in Forward Flight ($\mu = 0.3$).

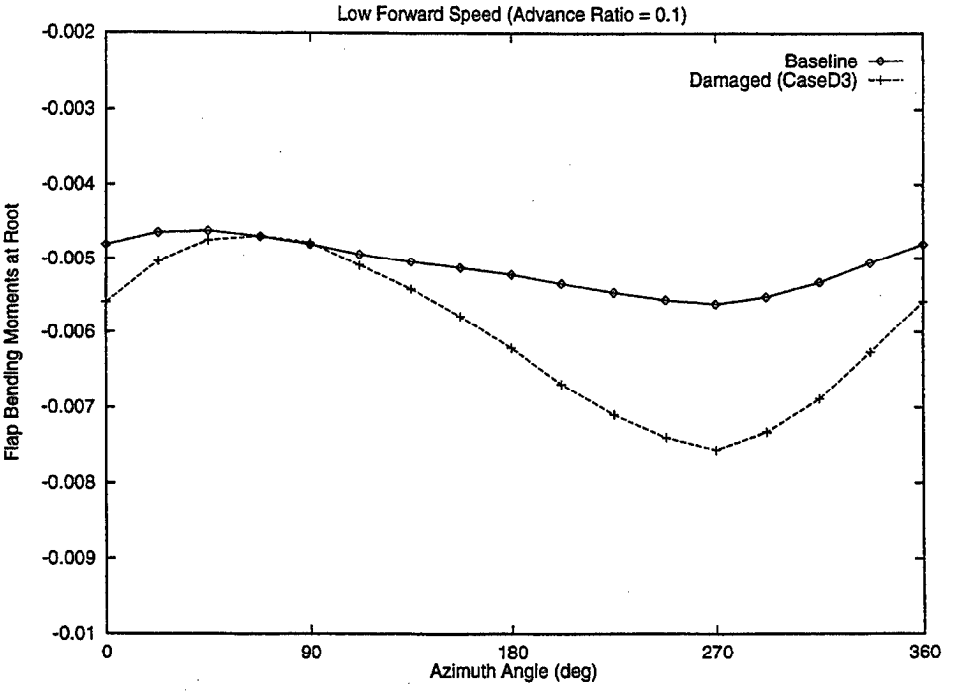

Figure 17. Flap Bending Moments of Undamaged and Damaged Blades in Forward Flight ($\mu = 0.1$).

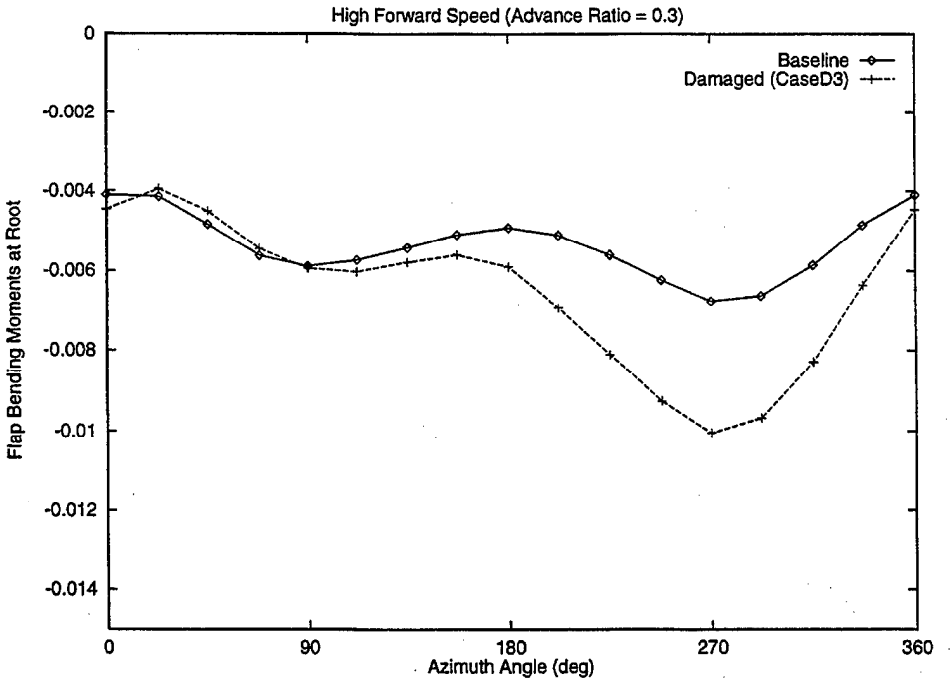

Figure 18. Flap Bending Moments of Undamaged and Damaged Blades in Forward Flight ($\mu = 0.3$).

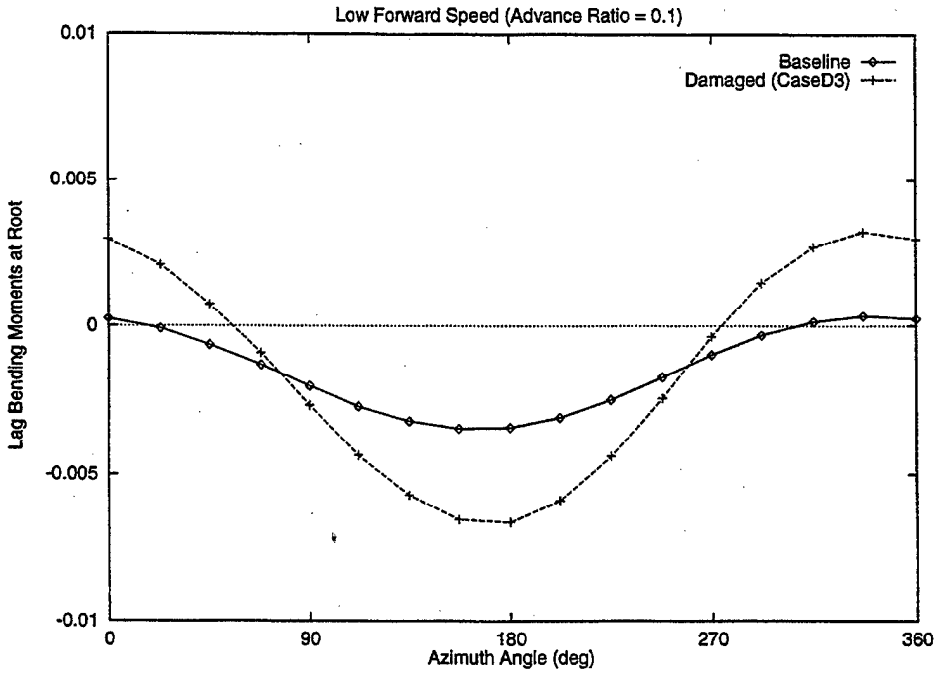

Figure 19. Lag Bending Moments of Undamaged and Damaged Blades in Forward Flight ($\mu = 0.1$).

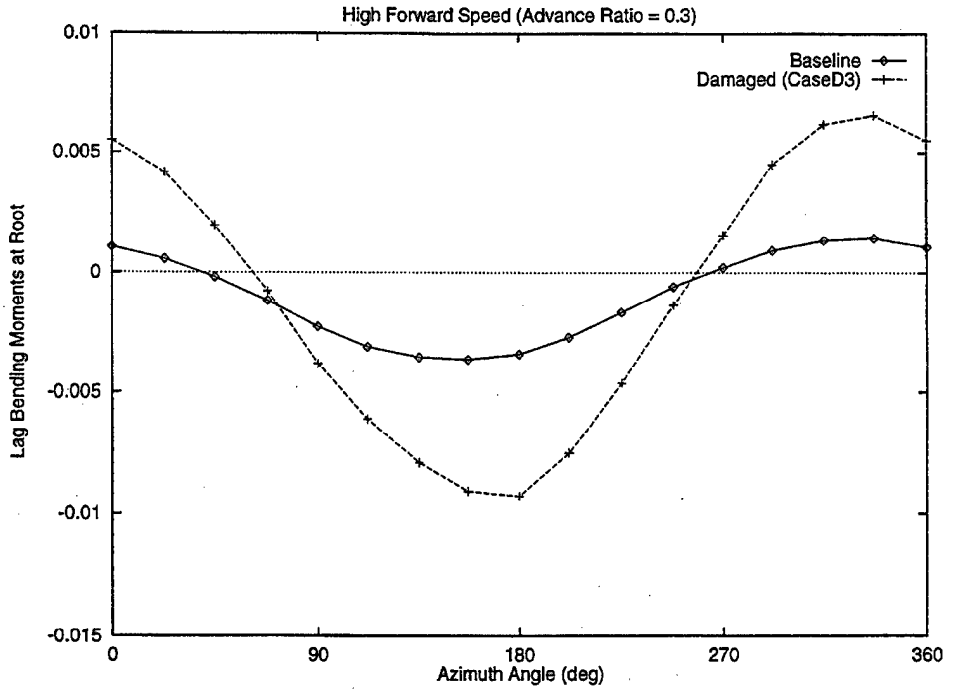

Figure 20. Lag Bending Moments of Undamaged and Damaged Blades in Forward Flight ($\mu = 0.3$).

4.4 Rotor Hub Vibrations

Hub loads and moments are calculated by summing the individual blade loads and transferring them to the fixed coordinate system. These hub forces and moments are transmitted to the fuselage and cause the vehicle vibrations. Therefore, the increase in hub loads will increase the vibration levels along the fuselage. In fact, the hub vibration level is a key indicator for assessing helicopter vibration level.**[3]**

The vibratory components of hub load and moment of the rotor system with and without blade damage are compared in Tables 8 and 9. The magnitude and harmonic contents of the in-plane hub load (F_x) and hub rolling moment (M_x) are shown for the baseline and three damage helicopters (CaseD1, CaseD2, CaseD3) in forward flight ($\mu = 0.3$). The hub force is nondimensionalized by $m\Omega^2R^2 10^{-3}$ and moment by $m\Omega^2R^3 10^{-4}$. One observes a predominant 4/rev vibratory component in hub vibrations with this four-bladed rotor for the undamaged (baseline) case. It is also seen that a helicopter with a ballistically damaged rotor blade is subject to other forcing frequency components than the nominal 4/rev vibration. In particular, the existence of the low harmonic vibratory components (1/rev and 2/rev) with the large amplitudes can be a significant factor influencing the flight performance of the vehicle. Also shown in the

tables is that the helicopter undergoes more severe vibrations when a blade is damaged out board toward the tip than in board. This is most likely because the rotor blade with outboard tip damage responds differently than the blade with in-board damage as compared to the baseline blade, as shown in the preceding results.

Table 8. Harmonic Analysis of Vibratory Hub Loads, F_x ($\mu = 0.3$)

Harmonics (per revolution)	Baseline	CaseD1	CaseD2	CaseD3
1		1.81	1.87	2.14
2		0.64	0.76	0.81
3		0.38	0.41	0.48
4	0.29	0.26	0.23	0.21
5		0.04	0.05	0.04
6		0.02	0.01	0.02

Table 9. Harmonic Analysis of Vibratory Hub Loads, M_x ($\mu = 0.3$)

Harmonics (per revolution)	Baseline	CaseD1	CaseD2	CaseD3
1		1.01	1.17	1.54
2		0.31	0.34	0.53
3		0.22	0.21	0.28
4	0.14	0.13	0.12	0.12
5		0.03	0.04	0.02
6		0.02	0.01	0.01

5. SUMMARY

Systematic investigation of rotor blade ballistic damage effects on helicopter vibrations was conducted using the UMARC comprehensive aeroelastic analysis. The analysis was based on finite element theory in space and time coordinates. The helicopter main rotor blades were modeled as a number of elastic beam finite elements, wherein each beam element undergoes flap bending, lag bending, elastic twist, and axial deflections. Aerodynamic forces on rotor blades were calculated using quasi-steady aerodynamic theory with a linear in-flow model. Ballistic damage was simulated as the span-wise distribution of mass, bending, and torsional stiffness change and aerodynamic characteristics change. Additionally, the effects of blade tip loss on the aeroelastic characteristics of the blades were examined. Multi-blade formulation is used to calculate the vibratory forces and moments acting on the hub fixed system. Results were

calculated for the baseline undamaged rotor system and for several blade damage conditions to quantify the effects on helicopter vibration.

The following conclusions are applicable to the particular damage conditions considered in the present study:

- Blade damage affected all the modes of the blade, and these effects were more distinct in the higher modes.

- Loss of blade tip increases the natural frequencies of the blade.

- When a blade is damaged, as in the case of a hole in the in-board sections, the natural frequencies of the blade decrease. The frequencies increase as the location of the hole damage is varied from in board to out board toward the tip.

- Blade flapping amplitude increases as the location of the damage is varied from in board to out board toward the tip.

- Blade dissimilarity induces a large 1/rev variation in the hub loads.

One must address other frequency components besides the pN_b/rev frequency forcing for the helicopter vibration study involving rotor blade damage. In particular, the existence of the low harmonics (1/rev and 2/rev) with the large amplitudes can be a significant problem to the flight worthiness of the vehicle as well as human tolerance of the troops on board.

REFERENCES

[1] Bir, G., I. Chopra, and K.C. Kim, et al. "University of Maryland Advanced Rotorcraft Code (UMARC): Theory Manual," Technical Report 92-02, Aerospace Engineering Department, University of Maryland, College Park, MD, May 1992.

[2] Johnson, W. "A Comprehensive Analytical Model of Rotorcraft Aerodynamic and Dynamics." NASA Technical Memorandum (TM) No. 81182, NASA Ames, CA, June 1980.

[3] Chopra, I. "Helicopter Dynamics and Aeroelasticity." Technical Notes, Center for Rotorcraft Education and Research, Aerospace Engineering Department, University of Maryland, College Park, MD, January 1991.

[4] Leishman, J.G. "Aerodynamic Characteristics of a Helicopter Rotor Airfoil As Affected by Simulated Ballistic Damage." ARL-CR-66, Army Research Laboratory Aberdeen Proving Ground, MD, September 1993.

[5] Leishman, J.G. "Experimental Investigation into the Aerodynamic Characteristics of Helicopter Rotor Airfoils with Ballistic Damage." ARL-CR-295, Army Research Laboratory Aberdeen Proving Ground, MD, April 1996.

[6] Kim, K.C. "Helicopter Trim Calculation in Forward Flight." Proceedings of the Summer Computer Simulation Conference, Society for Computer Simulation (SCS), Boston, MA, July 1993.

[7] Kim, K.C., and S.F. Polyak, "Evaluation of Helicopter Performance Degradation Due To Rotor System Damage." Proceedings of the Modeling and Simulation Workshop: Today and Tomorrow, International Test and Evaluation Association (ITEA), Las Cruces, NM, Dec 1995.

[8] MSC/NASTRAN Handbook for Aeroelastic Analysis Vol. 1. Los Angeles, CA: MacNeal-Schwendler Co., October 1987.

[9] Spyrakos, C. Finite Element Modeling in Engineering Practices, Pittsburgh, PA: Algor Inc., May 1995.

[10] Fries, J., and K.C. Kim, "The Effects of Helicopter Main Rotor Blade Damage on Fixed System Rotor Disk Vibration." Proceedings of the 20th Annual Meeting of the Vibration Institute, The Vibration Institute, St. Louis, MO, June 1996.

INTENTIONALLY LEFT BLANK

NO. OF COPIES	ORGANIZATION
2	ADMINISTRATOR DEFENSE TECHNICAL INFO CENTER ATTN DTIC OCP 8725 JOHN J KINGMAN RD STE 0944 FT BELVOIR VA 22060-6218
1	DIRECTOR US ARMY RESEARCH LABORATORY ATTN AMSRL CS AL TA REC MGMT 2800 POWDER MILL RD ADELPHI MD 20783-1197
1	DIRECTOR US ARMY RESEARCH LABORATORY ATTN AMSRL CI LL TECH LIB 2800 POWDER MILL RD ADELPHI MD 207830-1197
1	DIRECTOR US ARMY RESEARCH LABORATORY ATTN AMSRL DD J J ROCCHIO 2800 POWDER MILL RD ADELPHI MD 20783-1197
1	OUSD AT TWP ATTN GEORGE SCHNEITER RM 3E130 THE PENTAGON WASHINGTON DC 20310-3100
1	UNDER SEC OF THE ARMY DUSA OR1 RM 2E660 102 ARMY PENTAGON WASHINGTON DC 20310-0102
1	DEPUTY CHIEF OF STAFF OPERATIONS AND PLANS DAMO SW RM 3C6301 400 ARMY PENTAGON WASHINGTON DC 20310-0400
1	US ARMY TRADOC ANL CTR ATTN ATRC W WHITE SANDS MISSILE RANGE NM 88002-5502
1	US ARMY TRNG & DOCTRINE CMD ATTN ATCD B FT MONROE VA 23561

NO. OF COPIES	ORGANIZATION
	ABERDEEN PROVING GROUND
2	DIRECTOR US ARMY RESEARCH LABORATORY ATTN AMSRL CI LP (TECH LIB) BLDG 305 APG AA
1	US ARMY TECOM ATTN AMSTE TA RYAN BLDG
1	US ARMY AMSAA ATTN AMXSY D APG MD 21005-5071
1	US ARMY AMSAA ATTN AMXSY ST APG MD 21005-5071
1	DIRECTOR US ARMY RESEARCH LABORATORY ATTN AMSRL SL DR WADE BLDG 328 APG MD 21005-5068
2	DIRECTOR US ARMY RESEARCH LABORATORY ATTN AMSRL SL B MS W WINNER MS JILL SMITH BLDG 328 APG MD 21005-5068
24	DIRECTOR US ARMY RESEARCH LABORATORY AMSRL SL BD J A MORRISSEY S POLYAK J FRIES D LINDELL K KIM (20 CYS) BLDG 1068 APG MD 21005-5068
1	DIRECTOR US ARMY RESEARCH LABORATORY ATTN AMSRL SL BE D BELY BLDG 328 APG MD 21005-5068
1	DIRECTOR US ARMY RESEARCH LABORATORY ATTN AMSRL SL E DR STARKS BLDG 328 APG MD 21005-5068

NO. OF
COPIES ORGANIZATION

ABSTRACT ONLY

1 DIRECTOR
US ARMY RESEARCH LABORATORY
ATTN AMSRL CS AL TP TECH PUB BR
2800 POWDER MILL RD
ADELPHI MD 20783-1197

REPORT DOCUMENTATION PAGE

Form Approved OMB No. 0704-0188

Public reporting burden for this collection of information is estimated to average 1 hour per response, including the time for reviewing instructions, searching existing data sources, gathering and maintaining the data needed, and completing and reviewing the collection of information. Send comments regarding this burden estimate or any other aspect of this collection of information, including suggestions for reducing this burden, to Washington Headquarters Services, Directorate for Information Operations and Reports, 1215 Jefferson Davis Highway, Suite 1204, Arlington, VA 22202-4302, and to the Office of Management and Budget, Paperwork Reduction Project (0704-0188), Washington, DC 20503.

1. AGENCY USE ONLY *(Leave blank)*	2. REPORT DATE	3. REPORT TYPE AND DATES COVERED
	June 1999	Final

4. TITLE AND SUBTITLE

Analytical Investigation Into the Helicopter Vibration Resulting From Main Rotor Blade (MRB) Ballistic Damage

5. FUNDING NUMBERS

Project No. 1L162618AH80

6. AUTHOR(S)

Kim, K.C. (ARL)

7. PERFORMING ORGANIZATION NAME(S) AND ADDRESS(ES)

U.S. Army Research Laboratory
Survivability/Lethality Analysis Directorate
Aberdeen Proving Ground, MD 21010-5068

8. PERFORMING ORGANIZATION REPORT NUMBER

9. SPONSORING/MONITORING AGENCY NAME(S) AND ADDRESS(ES)

U.S. Army Research Laboratory
Survivability/Lethality Analysis Directorate
Aberdeen Proving Ground, MD 21010-5068

10. SPONSORING/MONITORING AGENCY REPORT NUMBER

ARL-TR-1985

11. SUPPLEMENTARY NOTES

12a. DISTRIBUTION/AVAILABILITY STATEMENT

Approved for public release; distribution is unlimited.

12b. DISTRIBUTION CODE

13. ABSTRACT *(Maximum 200 words)*

The effects of main rotor blade ballistic damage on helicopter vibration are investigated using a comprehensive helicopter aeroelastic analysis code. Ballistic damage to the rotor blade is represented in the blade structural model as well as in the aerodynamic analysis. Each blade is treated as being composed of elastic beams undergoing flap bending, lead-lag bending, elastic twist, and axial deflections. The dynamic response of mutli-bladed rotor systems is calculated from nonlinear periodic normal mode equations using a finite element in time scheme.

Results are calculated for a typical soft in-plane hingeless rotor helicopter with several damage configurations. Blade damage effects are determined in terms of blade mode shapes and frequencies, blade aeroelastic response, blade bending loads, and hub-fixed system vibration. Blade dissimilarity because of ballistic damage can induce a large vibratory component with its frequency the same as the rotor revolution (1/rev) on the helicopter system.

14. SUBJECT TERMS

aerodynamics, aeroelasticity, blade damage, blade dynamics, helicopter vibration

15. NUMBER OF PAGES

40

16. PRICE CODE

17. SECURITY CLASSIFICATION OF REPORT	18. SECURITY CLASSIFICATION OF THIS PAGE	19. SECURITY CLASSIFICATION OF ABSTRACT	20. LIMITATION OF ABSTRACT
Unclassified	Unclassified	Unclassified	